Journal of Sustainable Metallurgy (2020) 6:659–666
https://doi.org/10.1007/s40831-020-00301-7

RESEARCH ARTICLE

Low-Energy Feasibility for Leaching an Indigenous Scheelite Ore for Industrial Applications

Alafara A. Baba[1] · **John O. Kayode**[1] · **Mustapha A. Raji**[1]

Received: 2 September 2020 / Accepted: 5 October 2020 / Published online: 3 November 2020

Abstract

In recent times, the increasing demand for pure tungsten and its compounds in defense, medicine, high technology, and emerging innovations due to its excellent properties such as its tensile strength, corrosion resistance, and high modulus of elasticity cannot be overemphasized. In this study, an acid leaching route was adopted for the extraction of pure tungsten from a Nigerian scheelite ore consisting primarily of *scheelite* ($Ca_{4.00}W_{4.00}O_{16.00}$: 96-900-9627) and *quartz* ($Si_{6.00}O_{6.00}$: 96-900-5019). At optimal leaching conditions (2.5 mol/L HCl, 70 °C, < 75 µm), 88.5% of the initial 10 g/L ore reacted within 120 min. The low apparent activation energy (E_a) estimated as 22.94 kJ/mol with the reaction order of 0.96 affirmed the dissolution reaction to occur through the diffusion control mechanism of the first-order relation. The low E_a obtained further supports the feasibility and eco-friendly dissolution process as ~11.5% of the undissolved materials analyzed to contain silica (SiO_2: 96-900-5302) could be used as raw materials for some defined industrial applications.

Graphical Abstract

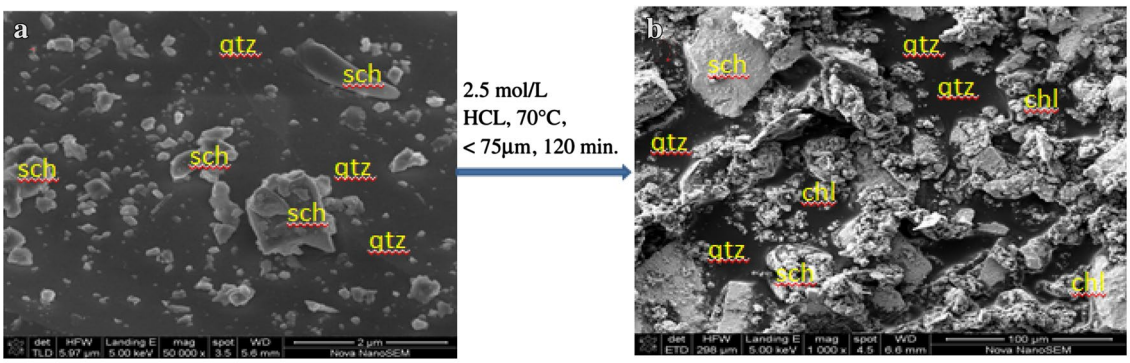

a: Raw scheelite ore; **b:** Residual product at optimal leaching conditions containing siliceous impurities; **sch:** scheelite; **qtz:** quartz; **chl:** calcium chloride

Keywords Scheelite · Wolframite · Leaching · Hydrochloric acid · Low activation energy

Introduction

Due to the global rise in population and economic growth, the need for the continuously increasing demand for many strategic and industrial metals that were previously not utilized in large quantities requires urgent attention, specifically, for such versatile raw materials including high-grade scheelite of industrial values whose supplies are important

The contributing editor for this article was U. Pal.

✉ Alafara A. Baba
baalafara@yahoo.com; alafara@unilorin.edu.ng

✉ John O. Kayode
kayjonny09@gmail.com

[1] Department of Industrial Chemistry, University of Ilorin, P.M.B. 1515, Ilorin 240003, Nigeria

to the human, defense, medicine, high-tech, and emerging innovations. This among others has prompted global attention by governments, industries, academics, and research agencies if the supplies of those versatile raw materials would satisfy the industrial demands or be tedious to obtain in the nearest future [1, 2].

In recent years, the continuous decline of high-grade tungsten ore deposits especially the low-grade tungsten ores such as wolframite, scheelite, and stolzite ores with an appreciable amount of tin has attracted the modern researchers [3, 4]. Tungsten, discovered by a Swedish chemist, Karl Wilhelm Scheele in 1781 [5], also referred to as wolfram, along with other transition metals such as chromium and molybdenum has five isotopes (W-180, W-182, W-183, W-184, and W-186) with the relative abundance of 30.64% W-184, 28.43% W-186, and 26.49% W-182, respectively [6].

However, tungsten as a strategic and industrial metal due to its excellent properties such as corrosion resistance, hardness, high modulus of elasticity, highest melting point, armaments, and tensile strength as well as vapor pressure makes its wide uses possible as a catalyst, cemented carbide, alloys and steels, lighting technology, electronics, X-ray tubes, and photo/electro-chromic usages [7–10]. According to the United States Geological Survey (USGS) statistical data in 2018, the world tungsten reserves including scheelite, wolframite, and its varieties are estimated to be around 3.3 million tons [11]. In Nigeria, for example, the wolframite ore deposits contain admixtures of scheelite and stolzite, which could be easily treated and beneficiated to obtain high-grade tungsten compounds of industrial utilities [7]. Nowadays, scheelite is the most common tungsten compounds with varied colors ranging from pale white to brown-orange, though dominated with blue coloration under UV, and often changes with increasing molybdenum content [7, 12].

For obtaining pure and high-grade scheelite products for industrial and manufacturing purposes, leaching techniques involving the ore in alkaline media such as sodium carbonate or sodium hydroxide by autoclaving [13–16] or acidic media such as hydrochloric acid [17, 18] or sulfuric acid [19, 20] to give tungstic acid (H_2WO_4) are mostly employed. Depending on the source of tungsten ores (wolframite, scheelite, or stolzite), various extraction routes are often used for purifying the leach liquor that arose from the leaching operations. For instance, the traditional processes of scheelite in acidic media include three underlisted *'win–win'* routes, Eqs. (1–3) [6]:

(i) Dissolution and leaching by hydrochloric acid or sulfuric acid to separate calcium as summarized in Eqs. (1) and (2):

$$CaWO_{4(s)} + 2HCl_{(aq)} \rightarrow H_2WO_{4(s)} + CaCl_{2(aq)} \quad (1)$$

$$CaWO_{4(s)} + H_2SO_{4(aq)} \rightarrow H_2WO_{4(s)} + CaSO_{4(aq)} \quad (2)$$

(ii) Extraction and purification of tungsten compound by ammonia solution as shown by the relation (3):

$$H_2WO_{4(s)} + 2NH_4OH_{(aq)} \rightarrow (NH_4)_2WO_{4(aq)} + 2H_2O_{(aq)}, \text{ and} \quad (3)$$

(iii) Evaporation and crystallization

The reaction mechanism of scheelite in alkaline media such as sodium hydroxide is represented by the following relation (4):

$$CaWO_{4(s)} + 2NaOH_{(aq)} \rightarrow Na_2WO_{4(s)} + Ca(OH)_{2(aq)}. \quad (4)$$

However, the scheelite ores treated with an alkaline solution appeared to be uneconomical due to the large volume of leachant and waste resources and often give rise to environmental pollution as a result of the release of toxic gases coupled with high intensive energy requirement during operation [21]. Moreover, the liquid waste emanated by these routes requires sophisticated equipment for processing the waste to meet the World Health Organization (WHO) Wastewater Discharge Standard [22].

Hence, to overcome the aforementioned setbacks, hydrochloric acid, owing to its cheapness, simple equipment design operation, and eco-friendly considerations, the treatment of indigenous scheelite mineral was examined in this study.

Materials and Method

Materials

The scheelite mineral used for this study was obtained from the Owa-Kajola axis, Ifelodun Local Government Area of Kwara State, Nigeria. The raw sample was crushed, ground, and sieved into three particle sizes: < 75 µm, 75 µm, and 90 µm, respectively. The smallest particle size (< 75 µm) assumed to have a larger surface area unless otherwise stated was used throughout the experiment. The hydrochloric acid (HCl) leachant used was of analytical grade and doubly distilled water was used in the preparation of all aqueous solutions.

Leaching Procedure

The leaching tests were performed in a 600 mL Pyrex leaching reactor equipped with a magnetic stirrer and a thermostat to control the reaction temperature. The hydrochloric acid solution at predetermined concentrations (0.1–2.5 mol/L) was added into the beaker and then heated to a preset

temperature at different leaching times (5–120 min). This was followed by adding 10 g/L of the < 75 µm scheelite smallest particle size to the reactor and the contents were thoroughly stirred. After a specific duration, the resultant solution was filtered, water-washed, and oven-dried at 40 °C for 24 h. The fraction of ore reacted in the leachant was calculated from the difference between the mass of the reacted and unreacted at various contact times after respective drying [7, 23, 24]. For a better understanding of the nature of the unreacted species, the residual product at optimal leaching conditions (2.5 mol/L HCl, 70 °C, < 75 µm, 120 min) was accordingly analyzed by X-ray diffraction (XRD) using PHILIP PW 1800 X-ray diffraction with Cu $K\alpha_1$ (0.154 nm) radiation graduated at 40 kV and 55 mA, Scanning electron microscopy (SEM) with NanoSEM 230, and Energy dispersive spectroscopy (EDS) with an oxford X-max EDS detector using INCA software, respectively. Also, the dissolution kinetics mechanism for the scheelite ore dissolution was determined by appropriate shrinking core models (SCM) [7, 23, 25].

Table 1 Chemical composition of raw scheelite by EDXRF

Compound	Composition (wt%)
WO_3	82.03
SiO_2	4.98
CaO	2.22
AuO	2.33
Fe_2O_3	0.25
Al_2O_3	0.45
P_2O_5	0.20
SO_3	0.31
ZnO	1.50
K_2O	0.02
Loss on ignition	3.2

The elemental composition of the major components of a Nigerian sourced scheelite ore examined by Skyray EDXRF 3600B Energy Dispersive X-ray fluorescence is summarized in Table 1.

The mineralogical purity by XRD analysis affirmed that the raw ore was made up of admixtures *scheelite* ($Ca_{4.00}W_{4.00}O_{16.00}$: 96-900-9627) and *quartz* ($Si_{6.00}O_{6.00}$: 96-900-5019) as the major attributed peaks as shown in Fig. 1.

However, the surface morphological of the scheelite ore under investigation by FEI Nova NanoSEM 230 equipment (Fig. 2) affirmed that tungsten-bearing scheelite is majorly associated with quartz impurities coupled with a polishing surface of the metallic phase.

Results and Discussion

Leaching Investigation

Effect of Hydrochloric Acid Concentration

The influence of hydrochloric acid concentration varying from 0.1 to 2.5 mol/L at a reaction temperature of 50 °C and

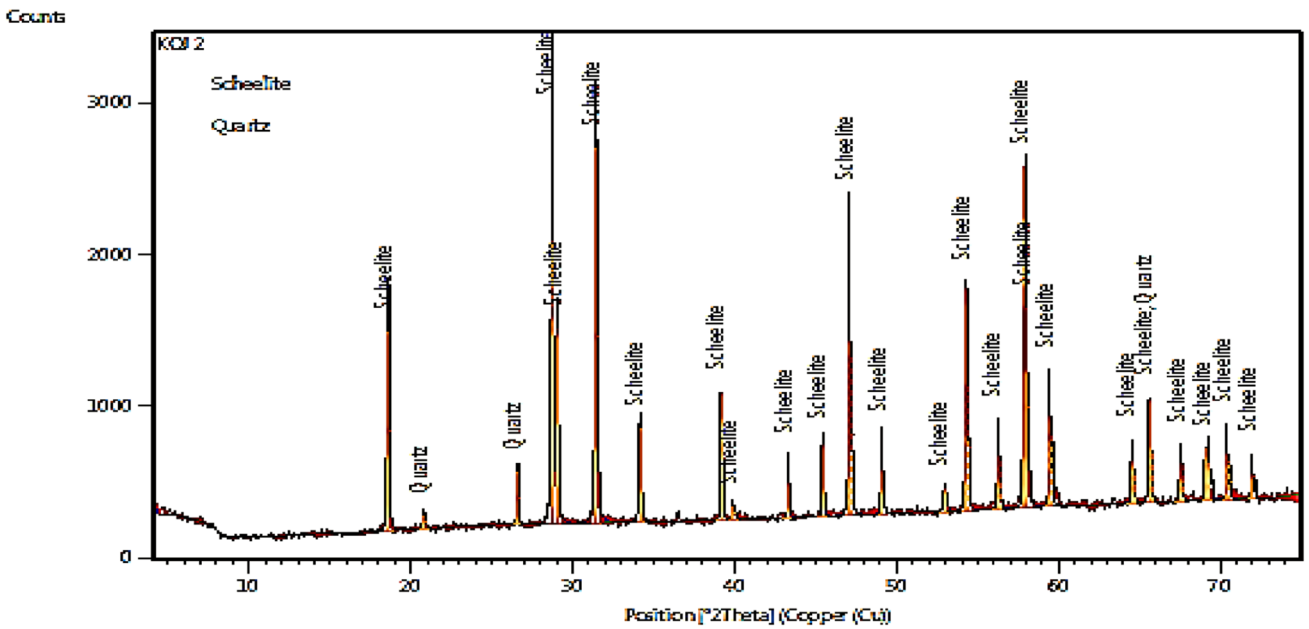

Fig. 1 X-ray diffraction of raw scheelite mineral

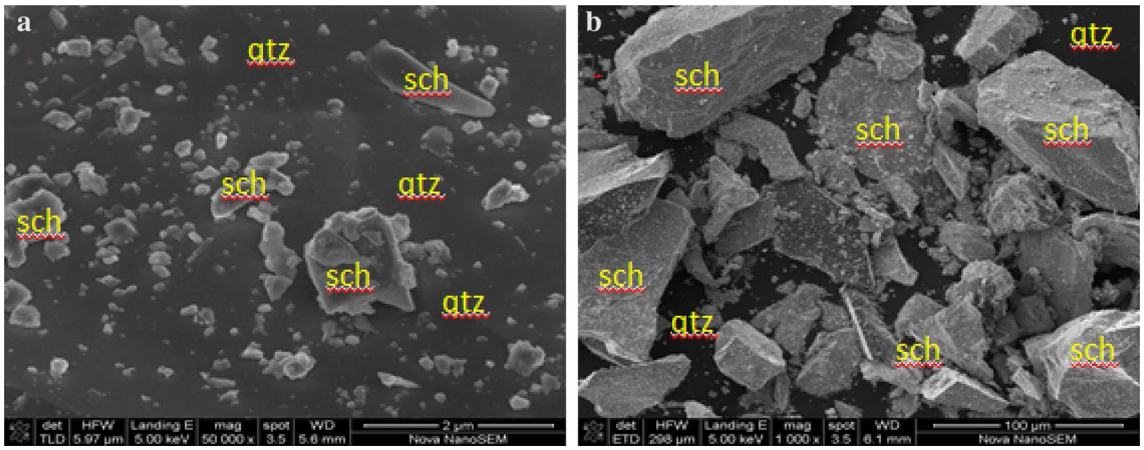

Fig. 2 SEM images of raw scheelite ore associated with quartz impurities (*sch* scheelite, *qtz* quartz)

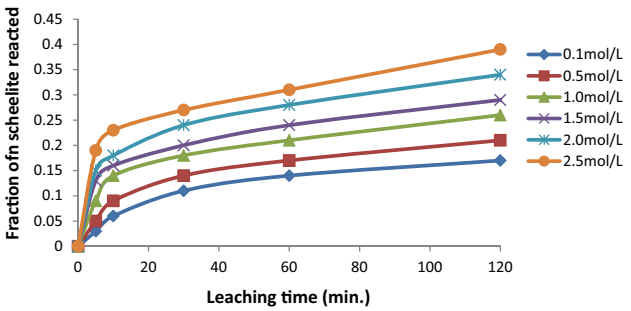

Fig. 3 Effect of hydrochloric acid concentration on the dissolution rate of the scheelite ore. Experimental conditions: [HCl] = 0.1–2.5 mol/L; reaction temperature = 50 °C; particle size = < 75 µm

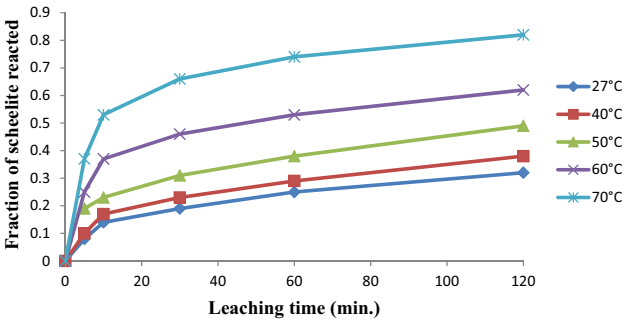

Fig. 4 Effect of reaction temperature on the dissolution rate of the scheelite ore. Experimental conditions: [HCl] = 2.5 mol/L; reaction temperature = 27–70 °C; particle size = < 75 µm

a particle fraction of < 75 µm on the dissolution efficiency of scheelite ore was examined. The results in Fig. 3 showed an increase in scheelite dissolution reaction with increasing hydrochloric acid concentration at various leaching times (Fig. 3).

For example, at 2 h of contact time, the dissolution reaction yielded 38.4% using 2.5 mol/L HCl solution, whereas the dissolution rate was 16.1% with 0.1 mol/L HCl solutions. This affirms that the concentration of hydrochloric acid has a considerable effect on the dissolution of scheelite ore which can be attributed to the presence of hydrogen [H^+] ion from hydrochloric acid solution [7].

Effect of Reaction Temperature

The influence of reaction temperature on the leaching reaction was investigated at 27–70 °C for the < 75 µm particle size by 2.5 mol/L HCl solution as depicted in Fig. 4.

The result in Fig. 4 shows that the reaction temperature had a spontaneous effect on the scheelite ore dissolution rate. At 70 °C, 88.5% of scheelite ore reacted within 120 min. However, at 27 °C, the dissolution efficiency decreased to 27.1% for 120 min and thereby confirmed that the reaction temperature significantly influences the possible complexation ability of hydrochloric acid [26]. Thus, the higher the reaction temperature, the faster the dissolution reaction.

Effect of Particle Size

The result on the influence of the particle fractions on the dissolution efficiency was investigated using the three particle fractions: < 75 µm, 75 µm, and 90 µm by 2.5 mol/L HCl solution and 70 °C reaction temperature as summarized in Fig. 5.

From Fig. 5, it is evident that the smaller ore particle diameter gave a faster dissolution rate. For instance, almost 89% of the scheelite reacted using the < 75 µm smallest particle diameter within 120 min, while the largest ore particle diameter gave 59.3% dissolution efficiency at optimal conditions. Thus, the finer the particle of the scheelite ore, the higher the dissolution rate, as the finer particle exhibited possible high surface properties.

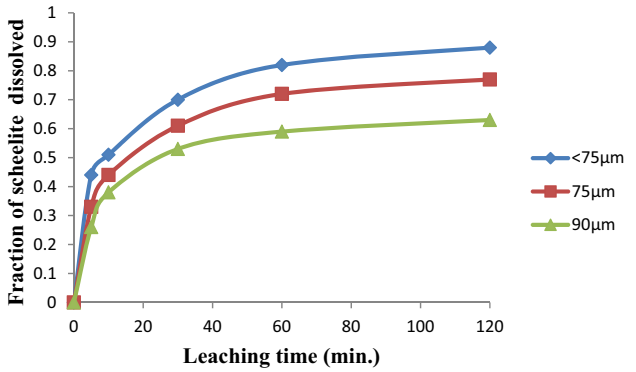

Fig. 5 Effect of particle size on the dissolution rate of the scheelite ore. Experimental conditions: [HCl] = 2.5 mol/L; reaction temperature = 70 °C; particle size = < 75–90 µm

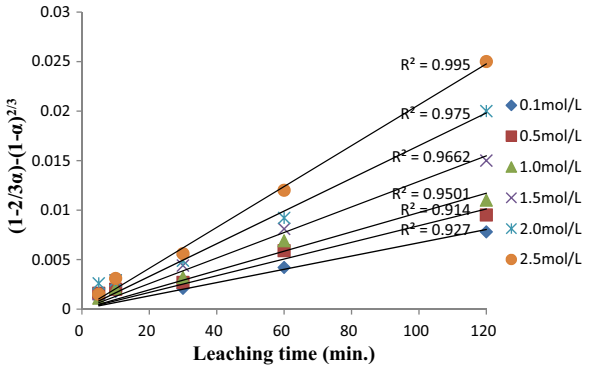

Fig. 6 A graph of $1-\frac{2}{3}\alpha-(1-\alpha)^{2/3}$ versus contact time at different acid concentrations. Conditions: Same as in Fig. 3

Discussion

Dissolution Kinetic Model

For a better understanding of the reaction mechanism exhibited by using scheelite ore with hydrochloric acid leachant in this study, it is mandatory to investigate its dissolution kinetic models using appropriate shrinking core models. However, two models vis-à-vis chemical reaction control and internal diffusion control equation models according to Eqs. (5) and (6) were employed [27, 28]:

$$1-(1-\alpha)^{1/3}=kt \quad \text{chemical control} \tag{5}$$

$$1-\frac{2}{3}\alpha-(1-\alpha)^{2/3}=kt \quad \text{diffusion control,} \tag{6}$$

where k is the specific rate constant (min^{-1}); t is the leaching time (min.); and α is the amount of fraction of the scheelite ore reacted at different leachant times, t (min). Consequently, the experimental data obtained from Figs. 3 and 4 were appropriately subjected to Eqs. (5) and (6) to determine the reaction order and activation energy for kinetic assessment through relevant Arrhenius plots. During the preliminary trials with the two appropriate models, it was found that only shrinking core model Eq. (6) fitted perfectly the dissolution data with the average correlation of $R^2=0.978>R^2=0.585$ using Eq. (5) model. Hence, the diffusion equation model (6) was used in the treatment of dissolution results in this study. For example, the dissolution data in Fig. 3 was treated with Eq. (6) to obtain the graph shown in Fig. 6.

The experimental rate constant, k, was estimated from Fig. 7 and the plot of ln k versus ln [HCl] gave the reaction order of 0.96, assumed to be the first-order relation.

However, the experimental data obtained from Fig. 6 were also substituted into Eq. (6) to obtain the plot affirmed in Fig. 8.

Also, the temperature dependence of the specific rate constant can be estimated from the Arrhenius expression:

$$k=A^{e-E_a/RT}, \tag{7}$$

where A is the frequency factor; k is the specific rate constant; E_a is the activation energy (J/mol); R is the universal gas constant (8.314 J/mol/K); and T is the absolute temperature (K).

Hence, Eq. (7) was linearized to obtain Eq. (8):

$$\ln k=\ln A-\frac{E_a}{RT}. \tag{8}$$

The activation energy, E_a, for the leaching reaction estimated from the slope of Fig. 9 gave 22.94 kJ/mol (< 40 kJ/mol), supporting the diffusion-controlled reaction

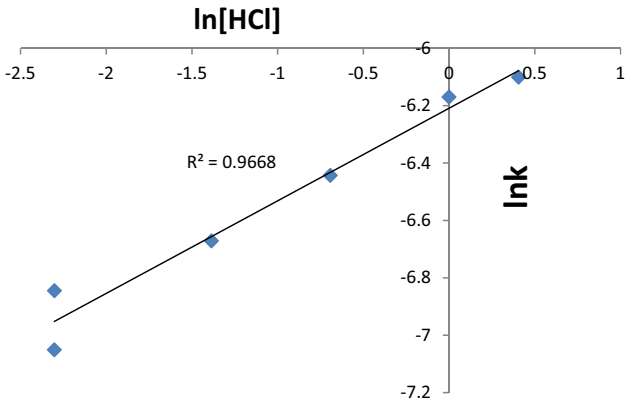

Fig. 7 A graph of ln k versus ln [HCl]. Conditions: Same as in Fig. 3

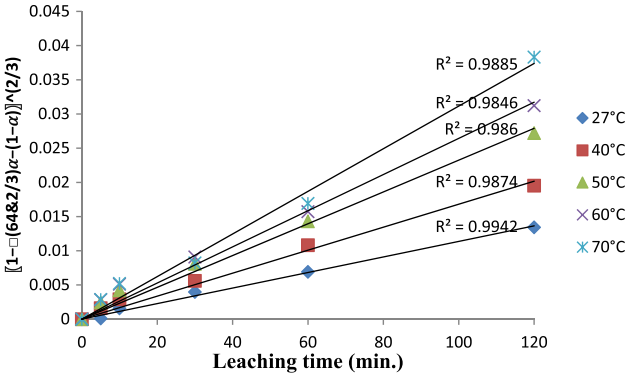

Fig. 8 A plot of $1-\frac{2}{3}\alpha-(1-\alpha)^{2/3}$ versus contact time at different reaction temperatures. Conditions: Same as in Fig. 4

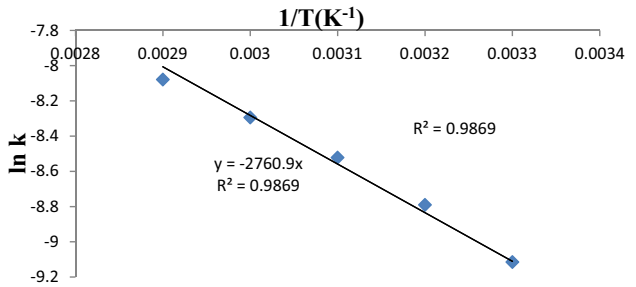

Fig. 9 A plot of ln k versus $1/T(K^{-1})$. Conditions: Same as in Fig. 8

mechanism as the rate-determining step for the dissolution reaction, consistent with the following stoichiometry [29–31]:

$$CaWO_{4(s)} + 2HCl_{(aq)}nH_2O \rightarrow CaCl_2.nH_2O_{(s)} + H_2WO_4, \quad (9)$$

and found to be kinetically more feasible with less activation energy as compared to other tungsten-bearing minerals from other sources (Table 2). The differences in the activation energies could be due to variation in geographical and environmental factors of the sourced materials.

Residual Product Analysis

The EDS analysis adopted to examine the elemental composition of the residual product at optimal leaching conditions (2.5 mol/L HCl, 70 °C, < 75 µm, 120 min) is depicted in Fig. 10.

Also, the morphological structure of the residue by SEM at optimal conditions is as shown in Fig. 11.

From Fig. 11, it is clear that the W-dominated region is bright due to the possible high atomic number and the bombardment of the leaching residue starts at the outer surface and then proceeds to the inner layer progressively [34]. However, the undissolved product (18.5%) analyzed by XRD was affirmed to majorly dominated by *scheelite* ($CaWO_4$: 96-900-7271) with few traces of *calcium chloride* ($CaCl_2$: 96-900-6902), and could, respectively, serve as valuable materials for some defined indigenous steel and coating industries.

Conclusion

Scheelite mineral has tremendously received the attention of global scientists due to being the major primary source of tungsten. Therefore, the development of effective and efficient routes for extraction and purification of tungsten from scheelite ores is pertinent for producing tungsten compounds of industrial value. Thus, in this study, the effects of leachant concentration, reaction temperature, and particle size on the optimization of scheelite ore dissolution were examined. The results affirmed that leachant concentration and reaction temperature strongly affect the ore dissolution. For instance, 88.5% of the ore reacted at optimal leaching conditions (2.5 mol/L HCl, 70 °C, < 75 µm) within 120 min. The experimental data obtained were subjected to the shrinking core model (SCM), where the diffusion-controlled reaction is the rate-determining step. The apparent activation energy was estimated to be 22.94 kJ/mol and supported the proposed reaction mechanism. Hence, the leaching kinetics via the established low activation energy prepared the indigenous scheelite ore used in this study for defined industrial applications.

Table 2 Activation energy feasibilities of tungsten-bearing minerals from different sources

Tungsten mineral	Sources	Conditions	Activation energies (kJ/mol)	References
Wolframite	Kazakhstan	95 °C, 0.5 h, S/L 15	243	Selivanov et al. [32]
Wolframite	Nigeria	1.5 mol/L HCl + 2.0 mol/L H_3PO_4, 75 °C	56.80	Baba et al. [7]
Scheelite concentrate	China	1.69–6.78 mol/L NaOH, 110 °C, 300–600 r/min	49.56	Li et al. [16]
Scheelite concentrate	China	50–400 g/L, 80 °C, − 74 + 58 µm	63.8	Li and Zhao [33]
Scheelite	Nigeria	0.1–2.5 mol/L HCl, 70 °C, < 75 µm	22.94	This study

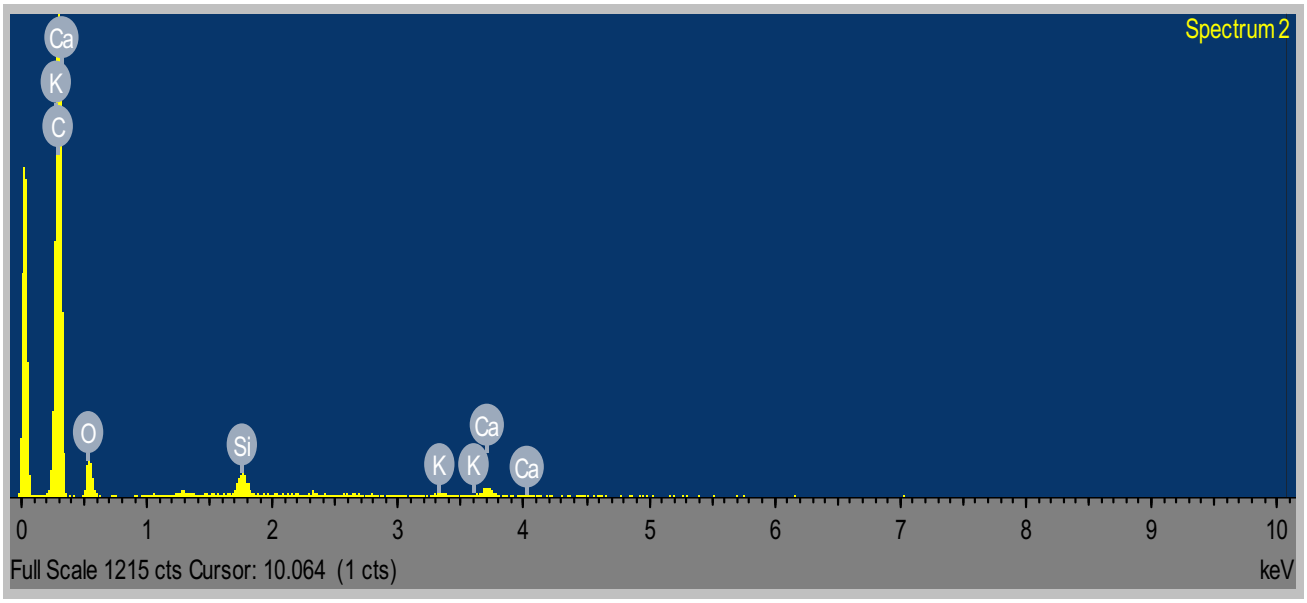

Fig. 10 EDS spectrum of the residual product at optimal conditions containing 77.59 wt% C, 20.89 wt% O, 0.59 wt% Si, 0.39 wt% K, and 0.54 wt% Ca

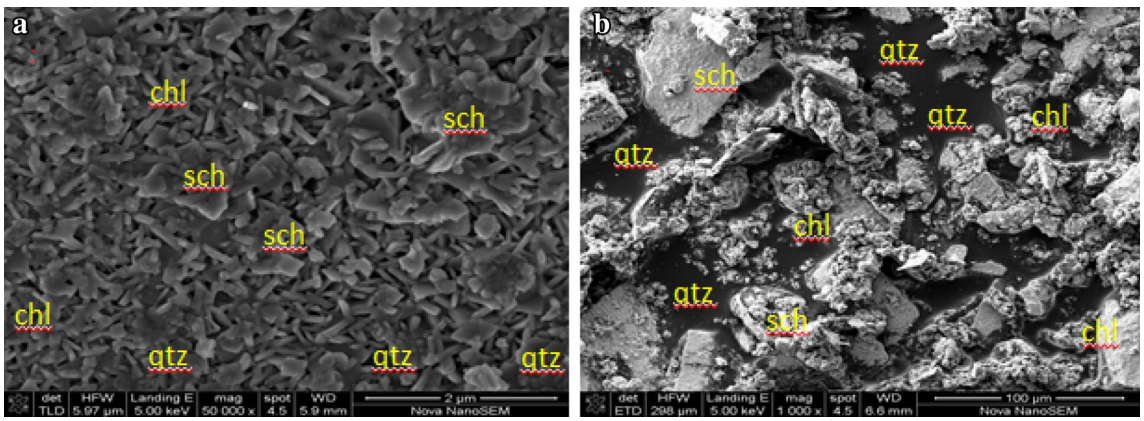

Fig. 11 SEM images of residual product at optimal conditions (**a** = 2 µm, **b** = 100 µm; *sch* scheelite, *qtz* quartz, *chl* calcium chloride)

Acknowledgement The authors gratefully acknowledge Miranda Waldron of the Centre for Imaging & Analysis, University of Cape Town, South Africa for assisting with SEM and EDX analyses.

Compliance with Ethical Standards

Conflict of interest The authors declare that there are no conflicts of interest.

Ethical Approval This article does not contain any studies involving human or animal subjects.

References

1. Shen L, Li X, Lindberg D, Taskinen P (2019) Tungsten extractive metallurgy: a review of processes and their challenges for sustainability. Miner Eng 142:105934
2. Tkaczyk AH, Bartl A, Amato A, Lapkovskis V, Petranikova M (2018) Sustainability evaluation of essential critical raw materials: cobalt, niobium, tungsten, and rare earth elements. J Phys D: Appl Phys 51:203001
3. He LH, Shen YJ, Peng J, Liu Q, Zhou XZ (2016) Extraction of tungsten from low-grade rough concentrate of tin and tungsten. Min Metall Eng 36(3):87–90

4. Wang YX, Dong HG (2015) Separation of tin and tungsten by selective leaching from high tin tungsten concentrate. Hydrometallurgy 34(1):17–20
5. Barabanov VF (1971) Geochemistry of tungsten. Int Geol Rev 13(3):332–344
6. Liu H, Nie C, Zhang J, Steenari BM, Ekberg C (2020) Comprehensive treatments of tungsten slags in China: a critical review. J Environ Manage 270:110927
7. Baba AA, Muhammed MO, Raji MA, Ayinla KI, Abdulkareem AY, Lawal M, Adekola FA, Alabi AGF, Bale RB (2018) Purification of a Nigerian wolframite ore for improved industrial applications. In: Rare metal technology 2018. Springer, Cham, pp 265–272
8. Sharma S, Taiwade RV, Vashishtha H (2017) Investigation on the multi-pass gas tungsten arc welded Bi-metallic combination between nickel-based superalloy and Ti-stabilized austenitic stainless steel. J Mater Res 32:3055–3065
9. Chen CI, Ma SH (2018) Study on characteristics and sintering behavior of W-Ni-Co tungsten heavy alloy by a secondary ball milling method. J Alloys Compd 731:78–83
10. Han FJ, Li FH, Liu SW, Niu L (2018) Sub-stoichiometric $WO_{2.9}$ as a co-catalyst with platinum for formaldehyde gas sensor with high sensitivity. Sens Actuators B Chem 263:369–376
11. USGS (2018) Tungsten statistics. US Geological Survey, Reston, VA
12. Pitfield P, Brown T, Gunn G, Rayner D (2011) Tungsten profile. British Geological Survey, London, p 34
13. Zhao ZW, Li JT, Wang XB, Li HG, Liu MS, Sun PM, Li YJ (2011) Extracting tungsten from natural scheelite with caustic soda by the autoclaving process. Hydrometallurgy 108(1–20):152–156
14. Zhao ZW, Liang Y, Liu XH, Chen AH, Li HG (2011) Sodium hydroxide digestion of scheelite by reactive extrusion. Int J Refract Metals Hard Mater 29(6):739–742
15. Queneau PB, Beckstead L, Huggins DK (1982) Autoclave soda digestion of natural scheelites with feedback control. US, US4325919.
16. Li T, Shen Y, Zhao S, Yin Y, Lu R, Gao S, Han C, Wei D (2019) Leaching kinetics of scheelite concentrate with sodium hydroxide in the presence of phosphate. Trans Nonferrous Met Soc China 29:634–640
17. Kalpakli AO, Ilhan S, Kahruman C, Yusufoglu I (2012) Dissolution behavior of calcium tungstate in oxalic acid solutions. Hydrometallurgy 121–124:7–15
18. Martins JI (2014) Leaching systems of wolframite and scheelite: a thermodynamic approach. Miner Process Extr Metall Rev 35(1):23–43
19. Li XB, Shen LT, Zhou QS, Peng ZH, Liu GH, Qi TG (2017) Scheelite conversion in sulfuric acid together with tungsten extraction by ammonium carbonate solution. Hydrometallurgy 171:106–115
20. Shen LT, Li XB, Zhou QS, Peng ZH, Liu GH, Qi TG, Taskinen P (2018a) Kinetics of scheelite conversion in sulfuric acid. JOM 70(11):2499–2504
21. Li HG, Li K, Yang JG (2011) Tungsten metallurgy. Central South University Press, Hunan, pp 2–5
22. Yin C, Ji L, Chen X, Liu X, Zhao Z (2020) Efficient leaching of scheelite in sulfuric acid and hydrogen peroxide solutions. Hydrometallurgy 192:105292
23. Shen L, Li X, Zhou Q, Peng Z, Liu G, Qi T, Taskinen P (2018b) Sustainable and efficient leaching of tungsten in ammoniacal ammonium carbonate solution from the sulfuric acid converted product of scheelite. J Clean Prod 197:690–698
24. Mohammadnejad S, Noaparast M, Hosseini S, Aghazadeh S, Mousavinezhad S, HosseinI F (2018) Physical methods and flotation practice in the beneficiation of a low-grade Tungsten-Bearing Scheelite Ore. Rus J Non-Ferrous Met 59(1):6–15
25. Sun F, Chen X, Zhao Z (2019) Synthesis of coarse-grained tungsten carbide directly from scheelite/wolframite by carbothermal reduction and crystallization. JOM. https://doi.org/10.1007/s11837-019-03345-7
26. Zhu X, Liu X, Zhao Z (2019) Leaching kinetics of scheelite with sodium phytate. Hydrometallurgy 186:83–90
27. Gong D, Zhou K, Li J, Peng C, Chen W (2019) Kinetics of roasting reaction between synthetic scheelite and magnesium chloride. JOM 71(8):2827–2833
28. Habibul N, Chen W (2018) Structural response of humic acid upon binding with lead: a spectroscopic insight. Sci Total Environ 643:479
29. Gong D, Zhou K, Peng C, He D, Chen W (2018) Resin-enhanced acid leaching of tungsten from scheelite. Hydrometallurgy 182:75–81
30. Xuin GH, Yu DY, Su YF (1986) Leaching of scheelite by hydrochloric acid in the presence of phosphate. Hydrometallurgy 16(1):27–40
31. Zhang W, Chen Y, Che J, Wang C, Ma B (2020) Green leaching of tungsten from synthetic scheelite with sulfuric acid-hydrogen peroxide solution to prepare tungstic acid. Sep Purif Technol 241:116752
32. Selivanov EN, Pikolin KV, Galkova LI, Gulyaeva RI, Petrova SA (2019) Kinetics and mechanism of natural wolframite interactions with sodium carbonate. Int J Miner Metall Mater 26(11):1364
33. Li J, Zhao Z (2016) Kinetics of scheelite concentrate digestion with sulfuric acid in the presence of phosphoric acid. Hydrometallurgy 163:55–60
34. Zhu X, Liu X, Zhao Z, Chen X, Li J, He L (2020) A green method for decomposition of scheelite under normal atmospheric pressure by sodium phytate. Hydrometallurgy 191:105234